INFLUENCE OF STRUCRURAL AND PHASE TRANSFOEMARION ON PROPERTIES OF SEVERELY DEFORMED DISPERSION-HARDENING ALLOYS

S.N. Faizova[1,2], I.A. Faizov[2], V.I. Semenov[3], F.F Hizbullin[1]

[1]Ufa State Petroleum Technological University
[2]Institute for Metals Superplasticity Problem RAS,
[3]ASI Institute for Strategic Studies, RB,Ufa,Russia
1 Kosmonavtov St., Ufa 450062 Russia
e-mail: snfaiz@mail.ru

Abstract: *The effect of severe plastic deformation on the kinetics of second phases in a dispersion-strengthening Cu-Cr-Zr alloy is investigated. The observed set of phenomena indicates that during SPD processing there occurs a complex interaction between deformation mechanisms and the processes of dissolution and precipitation of second-phase particles in the copper matrix, influencing structure refinement and resulting in a change of the particle sizes and their distribution, and consequently, the material's strength..*

Keywords: SEVERE PLASTIC DEFORMATION, ECAP, MICROSTRUCTURE, DISPERSION PARTICLES, STRAIN HARDENING, PHASE TRANSFORMATIONS

1. Introduction

Copper-rich dispersion-strengthening chromium bronzes are widely used, for example, for the production of resistance welding electrodes. In spite of a great variety of electrode designs, all of them are intended for the supply of current and pressing force to the welded parts, and for the removal of heat from the parts. This determines the main requirements to the material they are made of, i.e. high electrical conductivity and hardness (wear resistance).

The desired set of required functional properties in chromium bronzes can be attained due to structure refinement to the nanometer scale as a result of severe plastic deformation (SPD) processing. Materials produced by nanostructuring exhibit combinations of functional properties, different from those formed by conventional treatments [1-4]. Numerous studies have demonstrated that nanostructuring of conductive copper-rich chromium bronzes enables increasing significantly the mechanical characteristics of these alloys, preserving their high electrical and thermal conductivity [5-8].

The material under study belongs to the class of dispersion-strengthening materials, for which the morphology of second phases and the character of their distribution in the matrix plays an essential role in terms of the formation of the optimum combination of the basic functional properties (strength, thermal stability and electrical conductivity) in the material [5-8].

In the process of SPD, second-phase particles undergo a complex evolution involving their sizes, morphology and distribution in a material. The occurring changes are caused by both the mechanical fragmentation of particles and the deformation-induced phase transformations – particle dissolution and precipitation [5, 8-12]. Owing to a large density of dislocations and other structural defects, during SPD their spatial self-organization takes place, giving rise to considerable local inhomogeneities at the micro scale. This circumstance makes it possible to assume a simultaneous running of kinetically multidirectional processes of atom transport between second-phase particles and solid solution, which are correlated with the material's crystalline and defect structure. Second phases in the bronzes under study are an obstacle to dislocation motion, which creates an inverse effect of phase transformations on deformation, and consequently, on nanostructure formation.

Since the described phenomena are determined by a non-trivial interaction of processes having a different nature, their experimental study is associated with considerable difficulties and requires a comprehensive analysis of a wide range of non-uniform data. This work reports on the study of the evolution of second-phase particles ensemble and the associated change in the material's properties in the process of SPD and subsequent post-deformation ageing.

2. Materials and Methods

In the as-received state, the samples of the Cu-1Cr-0.7Al-0.2Zr alloy had the shape of rods with a diameter of 40 mm after standard industrial treatment. At the first stage – high-temperature treatment – the samples were subjected to holding for 1 hour at a temperature of 1050°C followed by water quenching in order to produce a solid solution of alloying elements in the copper matrix. Then the samples were subjected to cold deformation by equal-channel angular pressing (ECAP) followed by solid forging (SF) and drawing (D). Post-deformation ageing was performed at a temperature of 450°C for 1 hour. ECAP processing was conducted using a die set with a channels intersection angle of 90° via route Bc at room temperature, the number of ECAP passes was 8, the accumulated strain was e=1.1·8=8.8 [1-3]. Solid forging and subsequent drawing were conducted until the reduction of area reached 56% and 25%, respectively.

At all the stages, the material's structure was studied by optical metallography (OM), scanning electron microscopy (SEM), including EBSD analysis, transmission electron microscopy (TEM) –foils and extraction replicas.

To study in detail the changes in particle sizes and their distribution during SPD, the method of extraction replicas was used. Taking into account the specific features of the separation of particles from the matrix, the acquired statistical data on the particle sizes and distances between them may contain errors concerning the largest and the smallest sizes observed. However, considering the substantial statistics of conducted measurements, at least 1000 particles for each state, the character of changes in these values can be evaluated with sufficient assurance. The particle size was estimated as the average value of two measurements made in two mutually perpendicular directions.

The average distance between particles in a plane was calculated according to the formula: $L = \sqrt{\dfrac{S}{N}}$, where S is the sample surface area, N is the number of particles in the area S.

Study of the replicas by TEM made it possible to establish, while interpreting the electron diffraction patterns of individual particles, that the particles of certain compositions had a typical morphology. This fact was used for a further identification of particles, when statistical data were obtained.

Tensile mechanical test were performed on a universal Instron tensile testing machine at room temperature and a strain rate of 5.5×10^{4}s[-1], and Vickers microhardness measurements (under a

load of 1 N and a holding time of 10seconds) were conducted on Micromet 5101 microhardness tester.

At each stage of processing, the contributions of different strengthening mechanisms into offset yield strength were estimated.

3. Results and Discussions

The average grain size after the high-temperature treatment of the alloy is 34±3 μm, a noticeable amount of particles is observed. Since the average particle sizes in this state are rather small, their presence is evidently related to an insufficient quenching rate.

SPD processing (ECAP+SF+D) leads to a significant structure refinement – a banded, elongated along the rod, structure is formed (fig.1, a). The transverse size of fragments is about 200-240 nm.
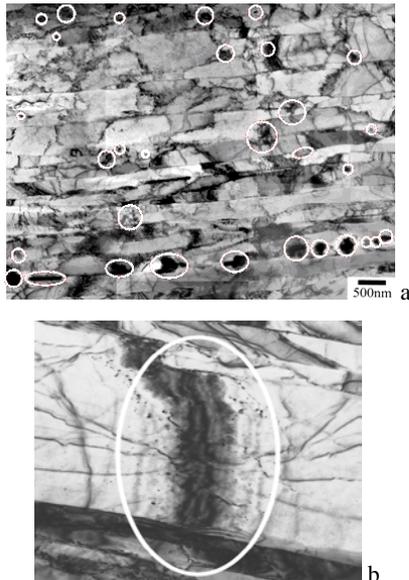

Fig.1 (a) Banded structure of the Cu-1Cr-0.7Al-0.2Zr alloy after a complex SPD processing. (b) Small particles are clearly visible in the grain close to the fringes of extinction.

The total density of particles decreases approximately two-fold as compared to the state after the high-temperature treatment. Although particles are observed both along boundaries and in grain interiors (fig.1, 2), worth noting is the correlation of their location with the features of defect structure and the fragment boundaries. A large number of small particles are observed, as a rule, in dislocation pile-ups.
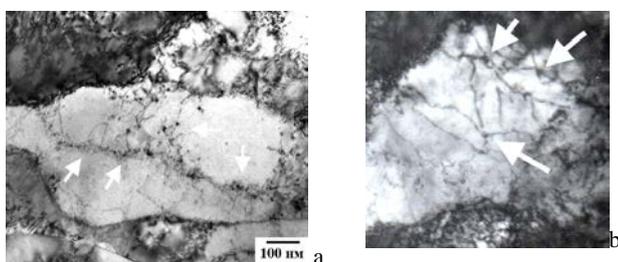

Fig.2. Interaction between particles and dislocations (a, b)

At the stage of post-deformation ageing, the transverse size of fragments has not changed, the observed density of second-phase particles has increased approximately by a factor of 4, as compared to the SPD-processed state, and the fraction of small, under 20 nm, particles has grown significantly.

Table 1 lists the average distances between particles, reflecting their distribution densities, estimated for the whole particle ensemble. In view of the variety of chemical compositions, the task to determine the changes in the number of particles for each of the ensemble components is beyond the scope of this work.

Table 1. Dependence of the average particle size and the average distance between particles on the processing stage

Processing stage	The average particle size, nm	The average distance between particles, nm
Initial	80	960
Solid solution treatment	40↓	460↓
SPD	50↑	680↑
Age hardening	20↓	360↓

At each stage of processing, the statistical characteristics of particle ensembles, differing in terms of their morphological features and chemical compositions, were identified.

Table 2 demonstrates how the average size of particles with different compositions changed at different stages of processing. Arrows show the direction in the changes of the average particle size.
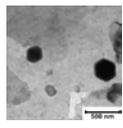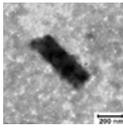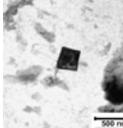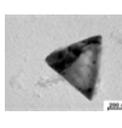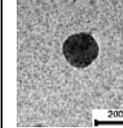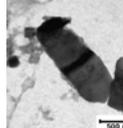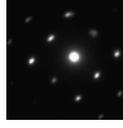
It can be seen from Table 2 that the average sizes of particles with different compositions change at the stage of SPD processing in different directions. After the high-temperature treatment, the copper-alumunium particles that were present in the as-received state, are not observed. They appear again after SPD processing, and in this state their average size is even larger than in the as-received state. Such a behavior unambiguously indicates the deformation-induced decomposition of solid solution in the process of SPD.

The revealed correlation between particles and the elements of the material's fragmented structure can be accounted for by the fact that particles, being efficient obstacles for dislocations (fig. 2, b), accumulate in their vicinity dense pile-ups, which are then transformed into fragment boundaries. An alternative mechanism, taking into account the presence of deformation-induced particle precipitation, could be that dislocation pile-ups and fragment boundaries are sinks for point effects and are therefore the preferred sites of new particles generation. In our opinion, most probable is the simultaneous synergetic action of both mechanisms.

At the same time, SPD causes a significant decrease in the total number of particles, which indicates the domination of the inverse process, namely, deformation-induced particle dissolution, closely related to their mechanical fragmentation [12]. Under this processing, the mechanical fragmentation of particles may take place only via quasi-brittle fracture, since the cutting of dislocations under the attained accumulated strains cannot play a significant role.

In terms of their composition, the particles are intermetallics having a crystal lattice incoherent with copper, as a result of which the particle/matrix interface is hardly permeable for dislocations. Being an obstacle for dislocation motion, a particle accumulates on itself a pile-up creating stresses, sufficient for the development of internal shears inside it, and eventually for its destruction.

Table 2. Changes in the average sizes of second-phase particles with processing stages in the Cu-1Cr-0.7Al-0.2Zr alloy. Each particle type is characterized by its typical morphology, electron diffraction pattern and chemical composition.

Particle types						
Processing stage	Cu_3Al, Cu_4Al, $CuAl$, Al_2Zr;	$ZrAl_3$, Zr_2Al_3, Cr	$ZrAl_2$, $Cu_{51}Zr_{14}$	AlCrZr.	Al_3Zr_5, Cu_5Zr, CuCr	$CuCr_4$
Initial state	125±4	98±4	88±5	83±4	60±4	96±5
Solid solution treatment	–	37±4 ↓	67±4 ↓	53±3 ↓	35±3 ↓	52±4 ↓
SPD	155±5	62±5 ↑	69±3	38±4 ↓	60±4 ↑	37±3 ↓
Age hardening	32±3 ↓	40±4 ↓	27±4 ↓	18±3 ↓	38±3↓	8±4 ↓

The formed fragments have areas with a high surface curvature (ribs), which makes thermodynamically possible their partial dissolution. The progress of dissolution is influenced by diffusion acceleration in the process of SPD [13]. The drift of impurity atoms in the field of dislocation pile-ups, relaxing after particle destruction, can also make a contribution into accelerated mass transfer. The efficiency of this process depends on the metastability degree of a specific intermetallic, which accounts for the complex changes in the sizes of particles of different compositions. The reduction in the average size of particles, caused by the dissolution process, makes some of them undetectable by TEM, which explains the observed decrease in their number after SPD processing.

Another indicator of kinetically multidirectional processes of dissolution and precipitation, running during SPD, can be the behavior of the lattice parameter of the copper matrix, depending on the concentration of the solid solution of alloying elements. Figure 3 shows the XRD data on the lattice parameter values after different numbers of ECAP passes, complete SPD processing and post-deformation ageing. It can be seen that this value changes non-monotonically. Since at the stage of deformation there are no grounds to expect the non-monotony of the contribution from stresses created by the defect structure, the main cause for such a behavior should be considered to be the changes in the concentration of solid solution as a result of phase transformations.
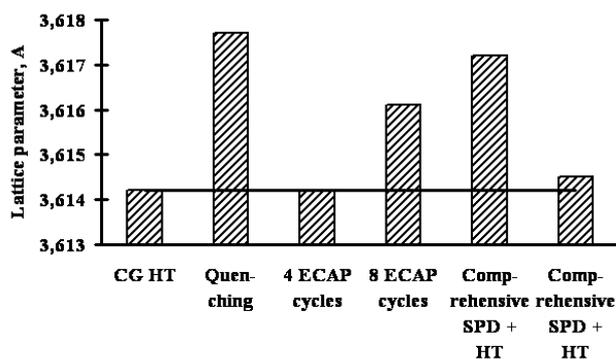

Fig.3. The copper lattice parameter of the Cu-1Cr-0.7Al-0.2Zr alloy at different stages of treatment

All of these changes indicate that under SPD there occur deformation-induced decomposition of solid solution and deformation-induced dissolution of second-phase particles.

Table 3. Mechanical properties of the alloy at different stages of processing

Processing stage	Microhardness, MPa	Tensile strength σ, MPa
Initial stage (after industrial treatment)	1450	**550**
Solid solution treatment	660	220
SPD	1400	550
Age hardening 450°C 1 h	1980	**700**

During post-deformation ageing, solid solution decomposition is finalized and, correspondingly, there appear many small, ~20 nm, particles, which determine eventually the high strength attained in this alloy – 700 MPa (Table 3). For comparison, after industrial treatment the average size of particles and the average distance between them is 80 and 960 nm, respectively, and strength is 550 MPa.

The high strength characteristics after a comprehensive processing of the alloy are possible only due to the interaction of two basic strengthening mechanisms – structural strengthening and dispersion strengthening. As demonstrated by the results described in this work, an important role in the interaction of these mechanisms is played by phase transformations observed under SPD.

Conclusions:

The obtained experimental results indicate that under the equal-channel angular pressing of chromium-zirconium bronze there occur not only refinement of the matrix structure, but also complex phase transformation involving the second-phase particle sizes and their distribution.

Analysis of the whole aggregate of experimental results, obtained at different structural levels, allows us to assume that two multidirectional processes are realized simultaneously: deformation-induced decomposition of the solid solution of alloying elements and deformation-induced dissolution of second-phase particles.

References

1. V.M. Segal. Mater. Sci. Eng. A 1995. V. 197. P. 157-164.
2. V.M. Segal, V.I. Reznikov, V.I. Kopylov, et al. Processing of Structure Formation in Metals. Minsk: Science and Technology, 1994. 231 p. (in Russian)
3. R. Z. Valiev, I. V. Alexandrov. Nanostructured Materials Produced by Severe Plastic Deformation. Moscow: Logos, 2000. 272 p. (in Russian)
4. R.A. Andrievski, A.M. Glezer. Physics – Uspekhi, 2009, Vol. 52, No. 4, P. 315–334. **DOI:** 10.3367/UFNe.0179.200904a.0337
5. S. Faizova, G. Raab, D. Aksenov, N. Zaripov, I. Faizov / Physical aspects of high-strength state formation in particle reinforced alloys under high pressure torsion // Fizicheskaya Mezomekhanika. Vol. 18, No. 4. 2015 (in Russian)
6. A. Vinogradov, V. Patlan, Y. Suzuki, K. Kitagawa, V. Kopylov. Acta Materialia. 2002. V.50, P.1639-1651. DOI: 10.1016/S1359-6454(01)00437-2
7. A. Vinogradov, T. Ishida, et al. Acta Materialia. 2005. V.53. P.2181-2192. DOI: 10.1016/j.actamat.2005.01.046
8. S. N. Faizova, R. Z. Valiev, N. V. Mazhitova, G. I. Raab. The kinetics of non-equilibrium solid solution of Cu-Cr during high-pressure torsion. Electronic journal "Phase Transitions, Ordered States and New Materials". 4. 2010. URL: http://ptosnm.ru/ru/issue/2010/4/49/publication/533 (in Russian)
9. V. V. Sagaradze, V. A. Shabashov, T. M. Lapina, et al. Low-temperature deformation-induced dissolution of Ni_3Al (Ti, Si, Zr) intermetallic phases in fcc Fe–Ni alloys. Phys. Met. Metallogr., **78**(6), 1994, 619-628.
10. V. V. Sagaradze, S. V. Morozov, V. A. Shabashov, L. N. Romashev, I. R. Kuznetsov. Dissolution of spherical and lamellar intermetallic compunds in Fe-Ni-Ti alloys during cold working. Fiz. Met. Metalloved. 66(2), 1988, P. 328-338. (in Russian)
11. V. A. Shabashov Nonequilibrium diffusion phase transformations and nanostructuring in intense cold deformation. Materials Science. 2008. No. 3(55). P. 169–179 (in Russian)
12. V. V. Sagaradze, Diffusion transformations in steels due to cold deformation, Metal Science and Heat Treatment, Vol. 50, No. 9-10, pp. 422-429, 2008.
13. Yu. R. Kolobov, R. Z. Valiev. Grain-boundary Diffusion and Properties of Nanostructured Materials // Novosibirsk: Nauka, 2001, 232 p. (in Russian)